

Supporting Information

High-Index Facet Gold 12 tip Nanostars for an Improved Electrocatalytic Alcohol Oxidation with Superior CO-tolerance

*Sanjeevan Rajagopal, Suresh Thangudu and Kuo Chu Hwang**

Department of Chemistry, National Tsing Hua University, Hsinchu 30013, Taiwan, R.O.C.

*E-mail: kchwang@mx.nthu.edu.tw

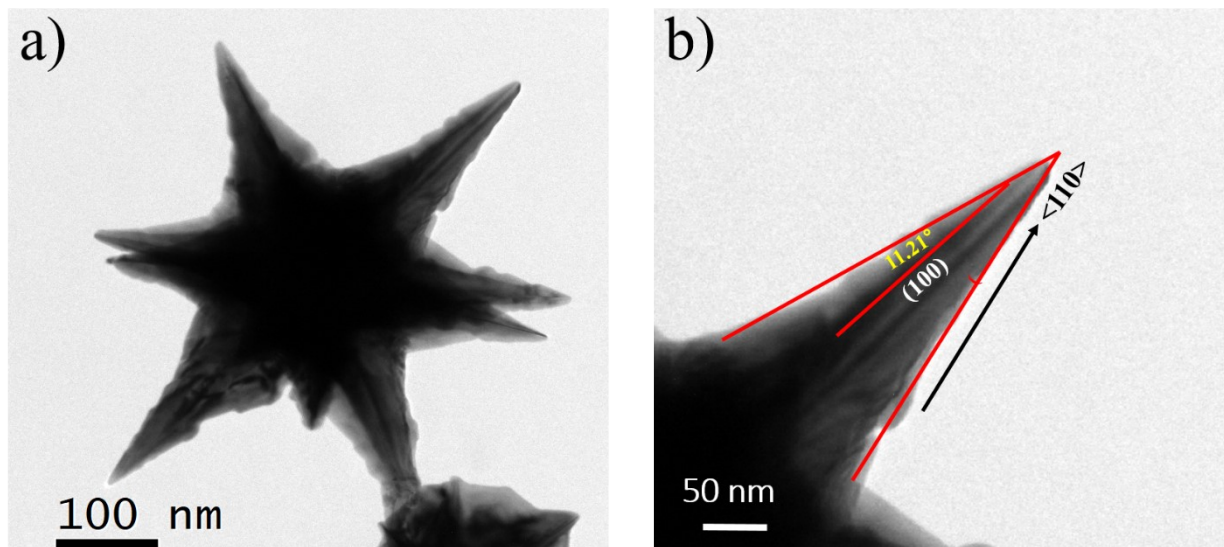


Figure S1. Au 12 tip nanostars. a) TEM image of a single nanoparticle. b) TEM images are taken from a single tip of the Au 12-tips nanostar shown in (a).

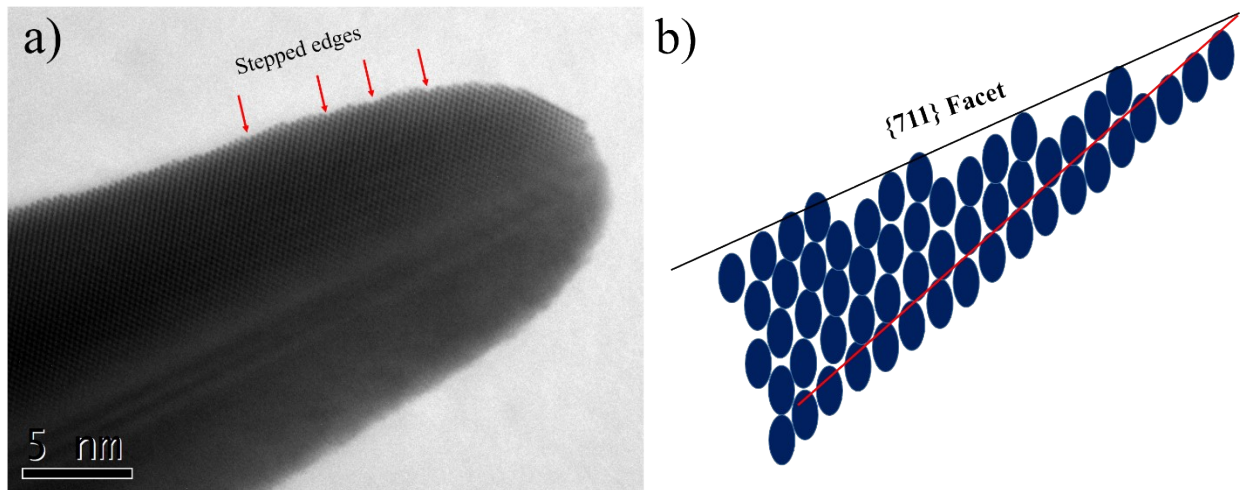


Figure S2. Au 12 tip nanostars. a) HRTEM images of the branches clearly illustrating the highly stepped edges. b) The theoretical atomic model of the {711} planes projected from the [-1, 1, 1] and [-1, 1, 0] zone axis and showing the (100) terraces and (111) steps.

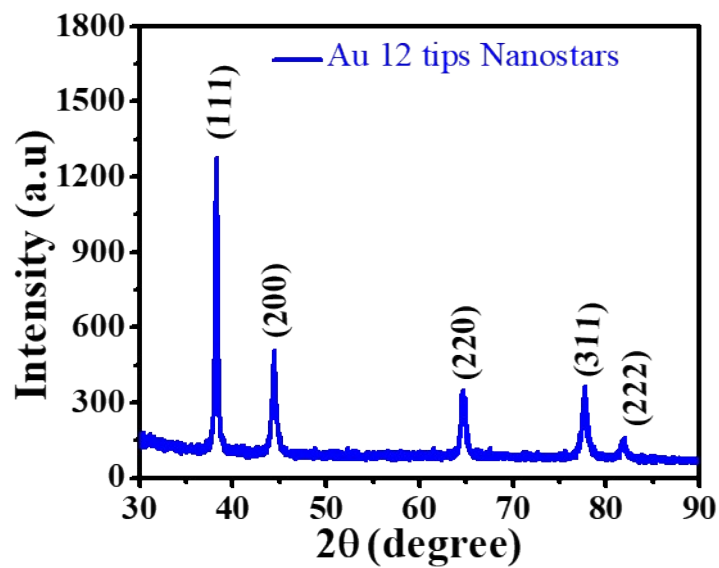


Figure S3. XRD pattern for Au 12 tips nanostructure.

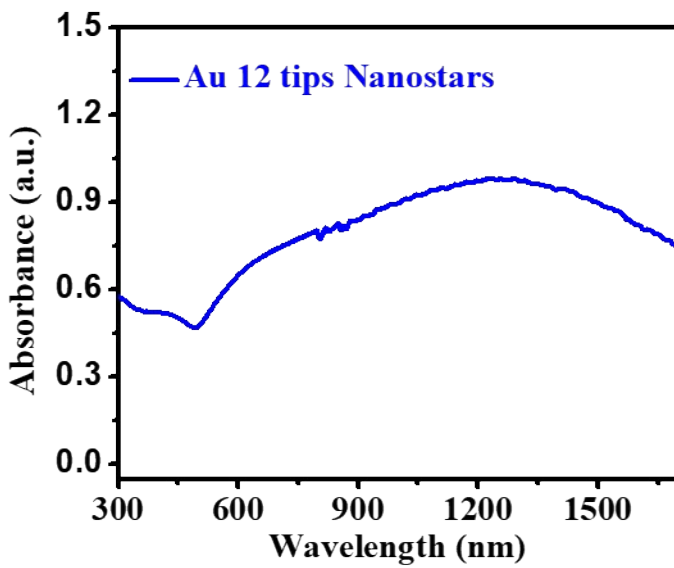


Figure S4. UV-Visible-NIR absorption spectrum of Au 12 tip nanostructure.

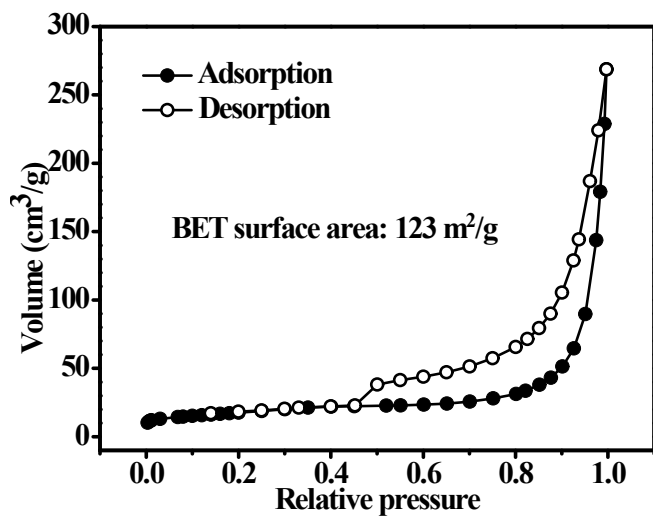


Figure S5. BET adsorption–desorption analysis of as synthesized Au 12 tips nanostars.

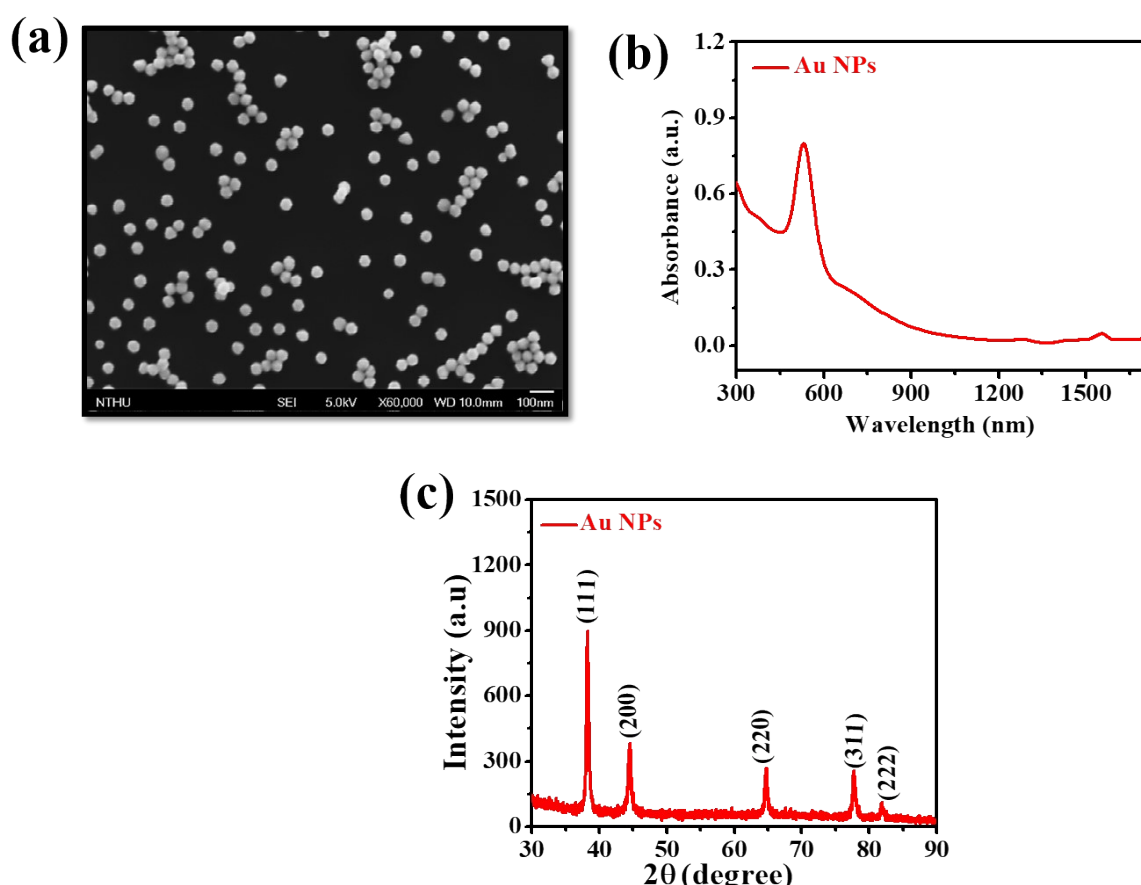


Figure S6. Characterization of Au NPs. (a) SEM image for Au NPs. (b) absorption spectra and (c) XRD of Au NPs.

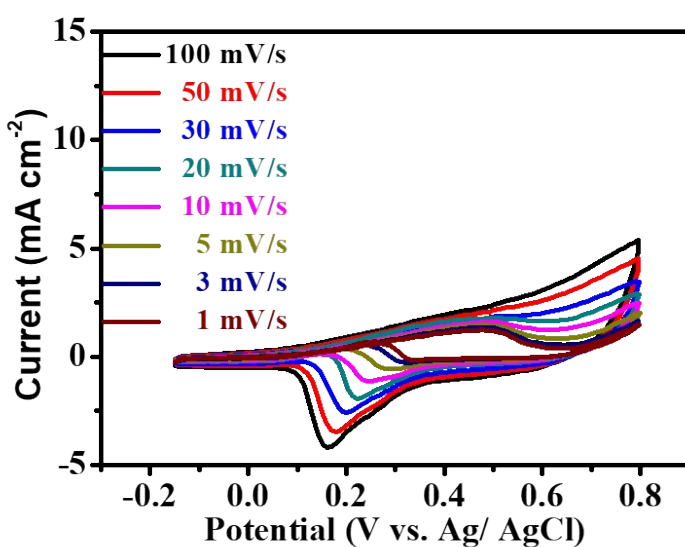


Figure S7. Cyclic voltammetry curves at a different scan rate effect with Au NPs, 0.5 M KOH, and 2 M methanol.

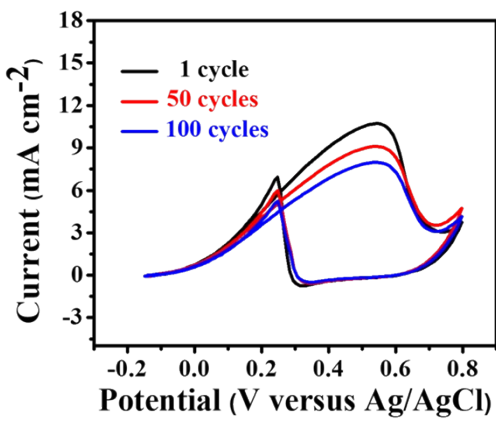


Figure S8. Electrocatalytic cycles in 0.5 M KOH electrolyte solution and 2 M methanol at a scan rate of 3 mVs^{-1} for 1- 100 cycles.

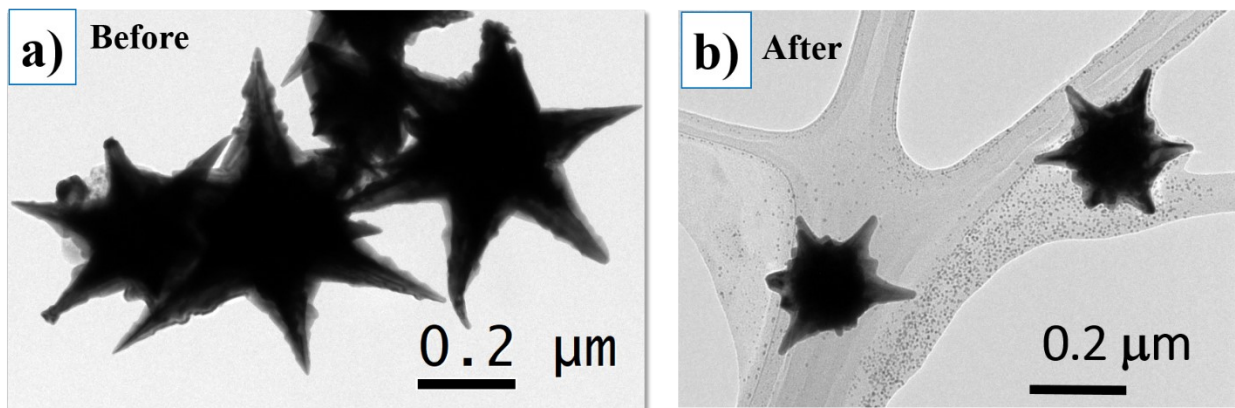


Figure S9. TEM images for Au 12 tips (a) Before the catalytic performance and (b) after catalytic performance.

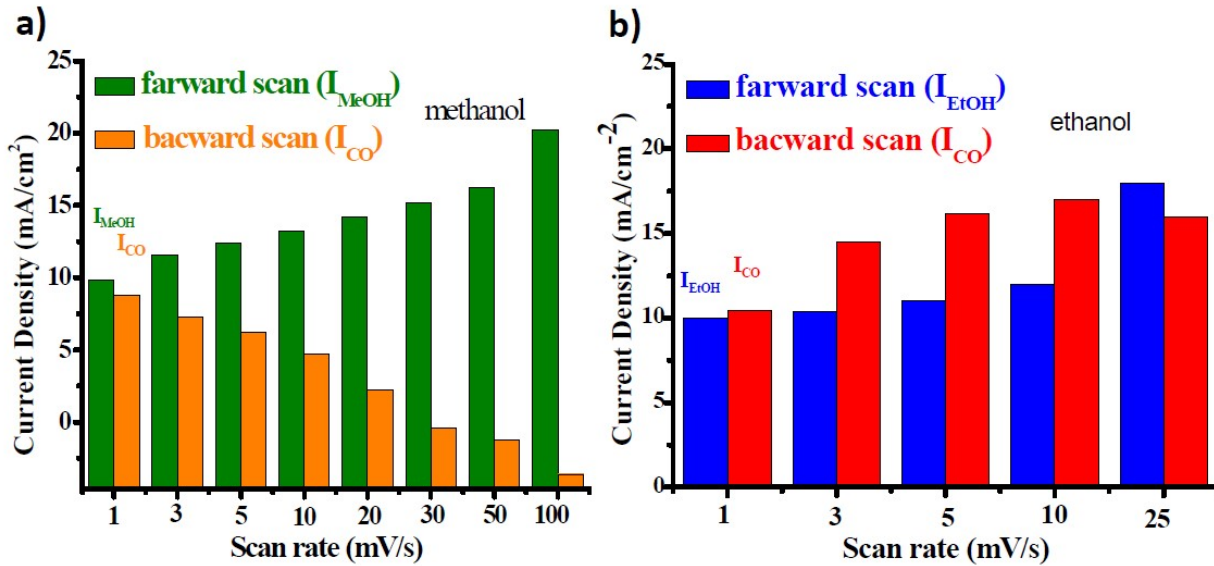


Figure S10. Forward and backward scan current densities for (a) methanol and (b) ethanol oxidations on Au 12 tips nanostars electrode, forward peak (I_f), backward peak (I_b).

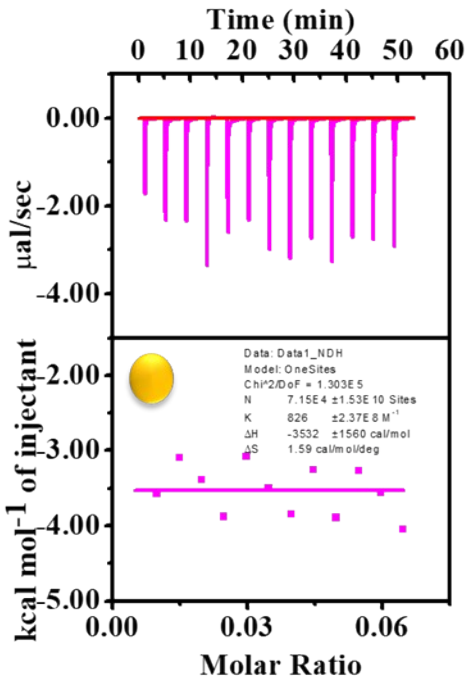


Figure S11. Isothermal titration calorimetry (ITC) titration curves on Au NPs electrode.

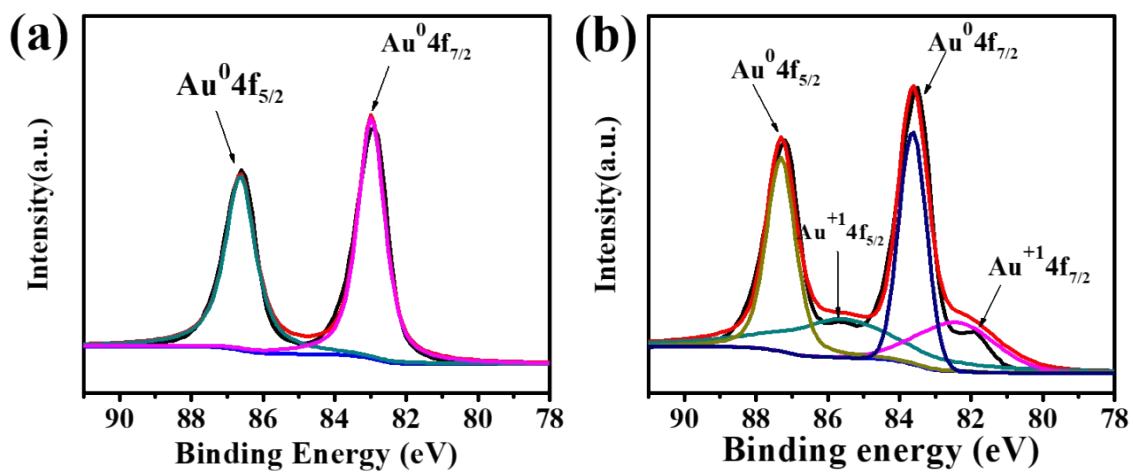


Figure S12. XPS spectra of Au 12 tip nanostars: a) before methanol oxidation reaction, and b) after methanol oxidation.

Table S1. Projection angles between (100) and (h11) facets.

Angle with {100}	55°	35°	25°	19°	15°	13°	11°
{h11}	{111}	{211}	{311}	{411}	{511}	{611}	{711}

Table S2. Summary of decreases in electrocatalytic activities of metal nanostructures for recently reported alcohol oxidation reaction.

Electrocatalysis	No. of Cycles	Scan Speed mV s ⁻¹	Catalysis decrease %	Reference
PtCu nanocubes	50	25	22.9	S1
Pd–WO ₂ .Nanosheets	50	50	21.1	S2
Pd-Ni alloy NPs	50	50	25.3	S3
NiCo ₂ O ₄ Nanoflowers	500	5	50	S4
Pt/C nanostructures	100	50	80	S5
Pt –Au NPs	7	10	85	S6
Au 12 tips nanostars	50	3	19	Present work
Au 12 tips nanostars	100	3	33	Present work

Table S3. Summary of ECSA and TOF values for recently reported electrocatalysts in methanol oxidation reaction

Electrocatalysis	Electrochemically Active Surface Area (ECSA) ($\text{m}^2 \text{ g}^{-1}$)	The turnover frequency (TOF) (s^{-1})	Reference
GC/Pd-PNMSS	29.15	0.0018	S7
Au NPs	0.50	0.0098	Current work
CuO/Co(OH) ₂ Nanosheets	8.5	0.255	S8
Au 12 tip nanostars	0.631	0.480	Current work
Pd ₆ Ru ₄ /TiO ₂ NPs	210	0.82	S9
Au–Pt alloy NPs	113	0.89	S10
Pt cubic nanoboxes	1.10	0.89	S11
Pt-Bi bimetallic NPs	539	1.37	S12

Table S4. Summary of ECSA and TOF values for recently reported electrocatalysts in ethanol oxidation reaction.

Electrocatalysis	Electrochemically Active Surface Area (ECSA) ($\text{m}^2 \text{ g}^{-1}$)	The turnover frequency (TOF) ($\text{atom}^{-1} \text{ s}^{-1}$)	Reference
Pd/C	21.1	0.20	S13
Hexagonal Pd/CNS	31.1	0.24	S14
Pd/RGO	19.5	0.33	S15
Pd-nitrogen-doped graphene	28.1	0.33	S13
Pd-polyaniline nanoparticles	66.0	0.36	S16
Au 12 tip nanostars	6.31	0.45	Current work
Pd/IL-RGO	23.6	0.58	S15

Supporting references

- S1. Y. Yang, Y. Guo, C. Fu, R. Zhang, W. Zhan, P. Wang, X. Zhang, Q. Wang and X. Zhou, *J. Colloid Interface Sci.*, 2021, **595**, 107–117.
- S2. L. Karuppasamy, C, Y, Chen. S, Anandan, S. and J, J, Wu, *ACS Applied Materials & Interfaces*, 2019, **11**, 10028-10041.
- S3. Sankar, G. M. Anilkumar, T. Tamaki and T. Yamaguchi, *ChemCatChem*, 2019, **11**, 4731–4737.
- S4. A, Y, Faid. H, Ismail, *ChemistrySelect*, 2019, **4**, 7896-7903.
- S5. P. Mehdipour, A. Omrani, H. Rostami and A. A. Rostami, *J. Mol. Liq.*, 2016, **219**, 165–172.

- S6. Y. Liu, Y. Zeng, R. Liu, H. Wu, G. Wang and D. Cao, *Electrochim. Acta*, 2012, **76**, 174–178.
- S7. F. Kaedi, Z. Yavari, M. Noroozifar and H. Saravani, *J. Electroanal. Chem.*, 2018, **827**, 204–212.
- S8. L. Chen, Z. Hua, J. Shi and M. He, *ACS Appl. Mater. Interfaces*, 2018, **10**, 39002–39008.
- S9. Y. Zheng, F. Chen, X. Liu, X. Guo, Y. Ying, Y. Wu, Y. Wen and H. Yang, *J. Power Sources*, 2020, **472**, 228517.
- S10. W. Ye, H. Kou, Q. Liu, J. Yan, F. Zhou and C. Wang, *Int. J. Hydrogen Energy*, 2012, **37**, 4088–4097.
- S11. Z. Peng, H. You, J. Wu and H. Yang, *Nano Lett.*, 2010, **10**, 1492–1496.
- S12. Y. Xiao, Y. Wang and A. Varma, *J. Catal.*, 2018, **363**, 144–153.
- S13. S. Li, J. Shu, S. Ma, H. Yang, J. Jin, X. Zhang and R. Jin, *Applied Catalysis B: Environmental*, 2021, **280**, 119464.
- S14. L. Karuppasamy. G, J, Lee, S. Anandan and J, J, Wu. *Applied Surface Science*, 2020, **519**, 146266.
- S15. S. Li. X, Liang. S, Shen, H. Yang, and C.M.L, Wu. *Inorganic Chemistry*, 2021, **60**, 17388-17397.
- S16. R, V, Jagadeesh, and V, Lakshminarayanan, *Applied Catalysis B: Environmental*, 2019, **251**, 25-36.